Science of the Total Environment 915 (2024) 170129

Contents lists available at ScienceDirect

Science of the Total Environment

journal homepage: www.elsevier.com/locate/scitotenv

Nano-selenium alleviates the pyroptosis of cardiovascular endothelial cells in chicken induced by decabromodiphenyl ether through ERS-TXNIP-NLRP3 pathway☆

Yangyang Jiang [a], Bowen Dong [a], Xing Jiao [b], Jianhua Shan [a], Cheng Fang [a], Kaixuan Zhang [a], Di Li [a], Chenchen Xu [a], Ziwei Zhang [a,c,*]

[a] College of Veterinary Medicine, Northeast Agricultural University, Harbin 150030, PR China
[b] China Institute of Water Resources and Hydropower Research, Beijing 100038, PR China
[c] Key Laboratory of the Provincial Education Department of Heilongjiang for Common Animal Disease Prevention and Treatment, PR China

HIGHLIGHTS

- Decabromodiphenyl ether (BDE-209) induced pyroptosis and inflammation in chicken cardiovascular endothelial cells.
- Inhibiting ERS revealed that BDE-209 causes vascular toxicity through the ERS-TXNIP-NLRP3 pathway.
- Nano-selenium can mitigate vascular injury and vasculitic response by BDE-209.

GRAPHICAL ABSTRACT

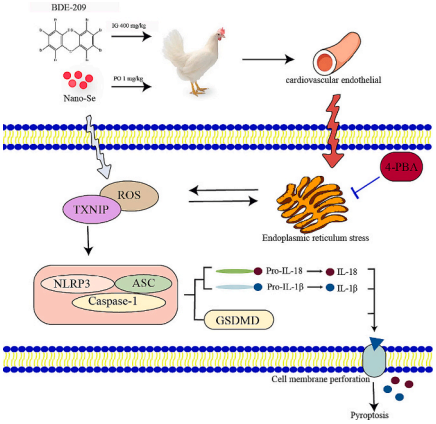

Abbreviations: BDE-209, decabromodiphenyl ether; Nano-Se, nano-selenium; ERS, endoplasmic reticulum stress; PAECs, chicken arterial endothelial cells; PBDEs, polybrominated diphenyl ethers; ECs, endothelial cells; ER, endoplasmic reticulum; UPR, unfolded protein response; ROS, reactive oxygen species; NLRP3, pyrin domain-containing protein 3; HAECs, human aortic endothelial cells; TXNIP, thioredoxin-interacting protein; Se, Selenium; CCK-8, Cell Counting Kit; H&E, hematoxylin and Eosin; SEM, scanning electron microscope; TEM, transmission electron microscope; DCFH-DA, 2,7-neneneba dichlorofluorescein diacetate; T-AOC, total antioxidant capacity; MDA, malondialdehyde; SOD, superoxide dismutase; CAT, catalase; IF, Immunofluorescence; GRP78, glucose regulatory protein 78; IRE1, inositol need enzyme 1; ATF6, activated transcription factor 6; CHOP, C/EBP homologous protein; PERK, protein kinase RNA-like kinase; ASC, apoptosis associated speck-like protein; PMSF, phenylmethane sulfonyl fluoride; SDS-PAGE, sodium dodecyl sulphate-polyacrylamide gel electrophoresis; PVDF, polyvinylidene fluoride; TRX, thioredoxin; CVDs, cardiovascular diseases; OS, oxidative stress.

☆ All authors have read the manuscript and agreed to submit it in its current form for consideration for publication in the Journal.

* Corresponding author at: College of Veterinary Medicine, Northeast Agricultural University, Harbin 150030, PR China.
E-mail address: zhangziwei@neau.edu.cn (Z. Zhang).

https://doi.org/10.1016/j.scitotenv.2024.170129
Received 26 September 2023; Received in revised form 8 January 2024; Accepted 11 January 2024
Available online 17 January 2024

ARTICLE INFO

Editor: Daqiang Yin

Keywords:
BDE-209
Nano-Se
Chicken arterial endothelial cells
Pyroptosis
Endoplasmic reticulum stress

ABSTRACT

Decabromodiphenyl ether (BDE-209) is one of the most widely used flame retardants that can infect domestic and wildlife through contaminated feed. Nano-selenium (Nano-Se) has the advantage of enhancing the antioxidation of cells. Nonetheless, it remains uncertain whether Nano-Se can alleviate vascular Endothelial cells damage caused by BDE-209 exposure in chickens. Therefore, we established a model with 60 1-day-old chickens, and administered BDE-209 intragastric at a ratio of 400 mg/kg bw/d, and mixed Nano-Se intervention at a ratio of 1 mg/kg in the feed. The results showed that BDE-209 could induce histopathological and ultrastructural changes. Additionally, exposure to BDE-209 led to cardiovascular endoplasmic reticulum stress (ERS), oxidative stress and thioredoxin-interacting protein (TXNIP)-pyrin domain-containing protein 3 (NLRP3) pathway activation, ultimately resulting in pyroptosis. Using the ERS inhibitor 4-PBA in Chicken arterial endothelial cells (PAECs) can significantly reverse these changes. The addition of Nano-Se can enhance the body's antioxidant capacity, inhibit the activation of NLRP3 inflammasome, and reduce cellular pyroptosis. These results suggest that Nano-Se can alleviate the pyroptosis of cardiovascular endothelial cells induced by BDE-209 through ERS-TXNIP-NLRP3 pathway. This study provides new insights into the toxicity of BDE-209 in the cardiovascular system and the therapeutic effects of Nano-Se.

1. Introduction

Polybrominated diphenyl ethers (PBDEs) are among the most widely used flame retardants and are incorporated into various textiles, polyurethane foams, electronic circuits and other material products (de Wit, 2002). Decabromodiphenyl ether (BDE-209) is a commercial form of PBDEs that is still heavily used in the global market. Moreover, during the production, usage, handling, or disposal processes, a substantial amount of BDE-209 is released into the environment (Wan et al., 2022). And due to their prolonged half-life and unstable chemical bonding properties, PBDEs persist in the air, soil and waters (Yu et al., 2016). The results of the multi-pathway exposure showed that the dietary pathway was still the primary exposure pathway for accumulating the PBDEs (approximately 65 % of the total exposure), the air was the second-largest exposure pathway (Wang et al., 2021a). Additionally, in chicken feed contaminated with PBDEs, the concentration of BDE-209 was found to be 80 %, surpassing other similar compounds (Wang et al., 2019). BDE-209 is accumulated significantly in terrestrial avian species, and residues of BDE-209 in poultry tissues and organs accumulate in the human body through the food chain (Chen and Hale, 2010). Over the past century, there has been an exponential increase of approximately 30-fold in the total amount of PBDEs found in human blood, tissues and milk (Hites, 2004). According to reports, the median concentration of BDE-209 in the blood of the general global population is 2.81 ng/g lw. In occupational groups, the maximum value reaches 521 ng/g lw, exceeding 180 times (Meng et al., 2021). Some animal experiments and human studies indicate that BDE-209 can cause damage to liver, kidney, testicles, mammary gland and other organs (Zhu et al., 2019; Li et al., 2014; Li et al., 2021; He et al., 2018). Additionally, it must be noted that persistent exposure to PBDEs in the circulatory system is associated with various cardiovascular diseases, such as hypertension, atherosclerosis and stroke (Lind et al., 2012). Xing's (Xing et al., 2018) research indicates that low concentrations of BDE-47 have adverse effects on early vascular development in zebrafish. Recent studies indicate that exposure to BDE-209 can induce oxidative stress (OS) and inflammatory responses in SD rats, leading to endothelial dysfunction and vascular damage (Jing et al., 2019). Although there are reports on the vascular toxicity of BDE-209, the specific mechanisms of its toxic damage to the chicken cardiovascular system are currently unclear and require further investigation. Our previous research indicates that BDE-209 can accumulate in various organs of poultry (Yang et al., 2022a; Zhang et al., 2023; Dong et al., 2023). Poultry products are also major meat products consumed by humans (Maharjan et al., 2021), and BDE-209 has potential toxic effects on humans, especially concerning the cardiovascular system (Zhi et al., 2018). Therefore, we investigated the cardiovascular toxicity of BDE-209 in chickens, aiming to elucidate its impact on the cardiovascular system of poultry. This experiment not only provides insights into the cardiovascular damage caused by BDE-209 in poultry but also serves as a reference for comparative medicine.

Endoplasmic reticulum (ER) is an organelle involved in protein synthesis, modification and folding in eukaryotic cells (Hetz et al., 2013). When protein homeostasis is out of equilibrium, cells restore balance by activating an unfolded protein response (UPR) (Li et al., 2020). But misfolded proteins accumulate in the ER leading to ER stress (ERS) (Chen et al., 2019). The homeostasis of the ER is closely related to normal cardiovascular function. ERS is both a cause and a consequence of various cardiovascular diseases (CVDs), including ischemic heart disease, hypertension, stroke, etc., creating a vicious cycle for these conditions (Ren et al., 2021). Some studies have indicated that BDE-209 can promote ERS. BDE-209 can promote apoptosis of mouse liver cells through ERS and mitochondrial dysfunction (Chen et al., 2022). The activation of the ERS-mediated Protein kinase RNA-like kinase (PERK) signaling pathway played a role in BDE-209-induced placental injury (Zhao et al., 2022). However, it is currently unclear whether ERS is associated with the chickens cardiovascular damage caused by BDE-209.

Pyroptosis is a pro-inflammatory mode of programmed cell death. It is characterized by the rapid rupture of the cell's plasma membrane, leading to the release of cellular contents and pro-inflammatory mediators (Li et al., 2023a). It plays a crucial role in the pathogenesis of various CVDs, such as human aortic endothelial cells (HAECs) and vascular smooth muscle cells (Pan et al., 2018). Its classical pathway is characterized by pyrin domain-containing protein 3 (NLRP3) inflammasome and caspase-1 activation, cell swelling and rupture, and release of IL-1β and IL-18 (Fang et al., 2020). NLRP3 inflammatorome stands as the most distinct inflammatory multiprotein complex in cells (Shao et al., 2015). It consists of NLRP3, apoptosis associated speck-like protein (ASC), and Pro-caspase-1. Activated Caspase-1 can recognize inactive pro-IL-1β and pro-IL-18 and convert them into mature inflammatory cytokines. It can also cleave members of the Gasdermin protein family, such as Gasdermin-D (GSDMD), leading to oligomerization of the final product GSDMD-N and mediating the formation of membrane pores (Sutterwala et al., 2006). ERS intersects with various inflammatory pathways, notably NLRP3 inflammasome (Ji et al., 2019). ERS can induce the generation of reactive oxygen species (ROS), leading to the dissociation of thioredoxin-interacting protein (TXNIP) from thioredoxin (TRX), thereby triggering the activation of the NLRP3 inflammasome (Oslowski et al., 2012; Lerner et al., 2012). Increasing evidence confirms that TXNIP promotes exacerbation of inflammatory responses through NLRP3 inflammasome-dependent mechanisms (Li et al., 2019). In preeclampsia, TXNIP is believed to play a crucial signaling role in linking ERS to the activation of the NLRP3 inflammasome, resulting in placental dysfunction (Yang et al., 2020). It is noteworthy that exposure to BDE-47 can activate ROS and the NLRP3 inflammasome, as well as the p38 MAPK pathway, in cochlear hair cells, leading to inflammatory responses and causing hearing damage (Tang et al., 2021). Similarly,

Jing's (Jing et al., 2023) research indicates that induction of pyroptosis and activation of NLRP3 inflammasomes in J774A.1 macrophage by Polybrominated diphenyl ether quinone (PBDEQ). However, whether BDE-209 can induce pyroptosis and inflammation in chicken cardiovascular tissue through the ERS-TXNIP-NLRP3 pathway remains uncertain.

Selenium (Se) is one of the essential trace elements for the human body with robust antioxidant capabilities (Cao et al., 2018). It serves a beneficial role in human and animal growth, neurobiology, reproduction and other aspects (Sun et al., 2023). Se is present in a range of selenoproteins, including key antioxidant enzymes expressed in endothelial cells (ECs), such as glutathione peroxidase and TRX reductase (Zheng et al., 2020). Therefore, vascular tissues are particularly sensitive to selenium deficiency (Chi et al., 2021), which can disrupt the homeostasis of vascular ECs (Cao et al., 2018). In recent years, nanotechnology has gained significant attention, and nano-selenium (Nano-Se), with its capacity to reduce toxicity and substantially enhance bioavailability, has emerged as a noteworthy development (Ge et al., 2022). Nano-Se has been widely used in various oxidative and inflammatory conditions, such as cancer and diabetes (Ge et al., 2021). Research has indicated that adding Nano-Se to chicken diets can enhance meat quality, improve immune function, and boost the antioxidant potential of chickens (Cai et al., 2012). Furthermore, Se has been found to mitigate renal OS and NLRP3 inflammasome damage induced by lead exposure (Huang et al., 2021). Therefore, the above studies emphasize that Nano-Se is expected to be a potential therapeutic agent for cardiovascular damage caused by BDE-209. Nevertheless, it is currently unclear whether Nano-Se can mitigate cardiovascular damage caused by BDE-209 and the specific underlying mechanisms.

In this study, the aim is to investigate the molecular mechanisms of BDE-209-induced vascular injury based on ERS and pyroptosis, and to explore whether Nano-Se can mitigate the vascular toxicity induced by BDE-209. Firstly, we conducted in vivo studies to investigate whether BDE-209 induces ERS and pyroptosis, and whether Nano-Se has inhibitory effects. Subsequently, cell experiments were performed to determine the specific molecular mechanisms. The use of ERS inhibitors was employed for intervention to elucidate the cellular pyroptosis mechanism induced by BDE-209. The in vivo and in vitro experiments demonstrate that BDE-209 exposure induces cardiovascular endothelial pyroptosis in chickens through the ERS-TXNIP-NLRP3 pathway. Additionally, it is clarified that Nano-Se alleviates cardiovascular damage induced by BDE-209 exposure by enhancing antioxidant capacity. This study provides a new perspective on the mechanism of cardiovascular damage caused by BDE-209 exposure and theoretical and experimental evidence for the mitigation of BDE-209 vascular toxicity by Nano-Se.

2. Materials and methods

All the methods used in this study were approved by Animal Care and Use Committee of Northeast Agricultural University (SRM-11).

2.1. Experimental animals and exposure protocol

A total of 60 healthy 1-day-old Hylanbai chickens were randomly allocated into four groups, each group had three replicates, each including five chickens: Control group, BDE-209 group, Nano-Se group and BDE-209 + Nano-Se group. The basic diet was provided using Dawei Chicken Pellet Feed 510 (Harbin, China). In the year 2000, the National Academy of Sciences in the US recommended an oral reference dose (RfD) of 4 mg/kg bw/d for commercial products containing BDE-209 (Goodman, 2009). At the same time, we also found that exposure of chickens to 400 mg/kg bw/d of BDE-209 can cause damage to the spleen (Cheng et al., 2022), kidneys (Sun et al., 2021), and liver (Yang et al., 2023). In earlier publications from our laboratory, Zhang (Zhang et al., 2023) demonstrated that exposure to 400 mg/kg bw/d of BDE-209 induces intestinal barrier damage and dysbiosis of the gut microbiota. BDE-209 (McLean Biochemical Co. LTD., Shanghai, China) was dissolved in corn oil and given 400 mg/kg by body weight gavage. Referring to Ge (Ge et al., 2021)'s research, Nano-Se (Jialong Nano Industry Co. LTD., Yantai, China) was incorporated into the feed at a ratio of 1 mg/kg. At the conclusion of the 42-day gavage period, all groups were euthanized and cardiovascular tissue was immediately collected. A portion of the samples was immersed in 4 % paraformaldehyde for subsequent experiments, while the other part was placed in liquid nitrogen for >1 h, and then stored in the refrigerator at −80 °C.

2.2. Cell culture and processing

Chicken arterial endothelial cells (PAECs) was derived from Animal Physiology research group of Northeast Agricultural University. RPMI1640 medium (Gibco, Shanghai, China) containing 10 % fetal bovine serum and 2 % chicken serum was prepared in advance for the culture of PAECs and placed in a humid incubator containing 5 % CO_2 at 37 °C. To assess the toxic effects of BDE-209 on PAECs, the Cell Counting Kit (CCK-8) reagent (BioSharp, Hefei, China) was employed. Various concentrations of BDE-209, including 50 μmol/L, 100 μmol/L, 200 μmol/L, 300 μmol/L and 400 μmol/L, were used. A 96-well plate was utilized, with each well containing 100 μL of cell suspension (1×10^6 cells/mL). Following a 12-h exposure to various concentrations of the BDE-209 solution, the medium was replaced with fresh medium containing 10 % CCK-8 working solution. The cells were subsequently incubated for 30 min, and the absorbance was measured at 450 nm using a microplate reader from TECAN in Switzerland. Similarly, CCK-8 cell viability assay was also performed to determine the effects of Nano-Se and 4-PBA (MedChemExpress, Shanghai, China) on cell activity. Finally, 5 experimental groups were set up in this study: NC group (normal control group), BDE-209 group (BDE-209:100 μmol/L), and BDE-209 + Nano-Se group (BDE-209:100 μmol/L, Nano-Se: 4 μmol/L), BDE-209 + 4-PBA group (BDE-209:100 μmol/L, 4-PBA: 0.5 mmol/L), BDE-209 + 4-PBA + Nano-Se (BDE-209:100 μmol/L, Nano-Se: 4 μmol/L, 4-PBA: 0.5 mmol/L).

2.3. Hematoxylin and eosin (H&E) staining

The preserved cardiovascular tissues were processed following the method outlined by Cai et al. (2021): they underwent dehydration using a series of ethanol gradients, followed by embedding in paraffin. Subsequently, 5 μm thick sections were sliced. These sections were then subjected to dewaxing and hydration processes. H&E staining was executed, and the samples were observed and photographed using an optical microscope from Nikon, Japan.

2.4. Electron microscopy

According to Zhang et al.'s (2021) method, the samples underwent sequential treatments with PBS, gradient ethanol, and tert-butanol. After the drying and application of a metalizing film, microscopic images of the chicken cardiovascular tissue were acquired using a scanning electron microscope (SEM) (Hitachi Limited SU8010, Japan). According to Zheng et al. (2021a), the specimens were initially fixed using glutaraldehyde and 1 % osmic acid. Subsequently, they were subjected to sequential treatments with PBS, gradient ethanol, acetone, and an embedding solution. The samples were then sliced and observed using a transmission electron microscope (TEM) (Hitachi Limited H-7650, Japan).

2.5. ROS staining

The intracellular level of ROS was assessed using a test kit from Beyotime (Shanghai, China). According to Cai et al.'s (2023) method, Cells from each group were incubated in a 2,7-neneneba dichlorofluorescein diacetate (DCFH-DA) medium (10 μM/mL) at 37 °C for 30

min. Then, the culture medium was sucked, the cells were repeatedly blown with PBS, and the cell suspension was collected into a 1.5 mL centrifuge tube. 1000 rpm/min, 5 min, after absorbing the supernatant, PBS was added to re-suspend the cells for determination. Subsequently, the cells were rinsed and visualized under a fluorescence microscope (Thermo Fisher Scientific, USA). The fluorescence signals indicative of ROS were then quantified utilizing Image J software.

2.6. Detection of antioxidant function

Accurately weigh 0.1 g of cardiovascular tissue, add 0.9 mL of normal saline, and homogenate and the homogenate was made by High speed low temperature tissue grinding machine (KZ-III-F) (Servicebio, Wuhan, China). Then centrifuge 2500 r/min for 10 min and take the supernatant to be measured. PAECs cells were cultured to 90 %, digested, centrifuged, the supernatant was discarded, leaving the cell layer, and PBS was added to make homogenate with Ultrasonic homogenizer (JY92-IIN) (Scientz, Ningbo, China), to be tested. The homogenate protein concentration was determined by total protein quantitative assay kit (JianCheng Bioengineering, Nanjing, China). The total antioxidant capacity (T-AOC), malondialdehyde (MDA), superoxide dismutase (SOD), and catalase (CAT) levels in both cardiovascular tissues and PAECs were quantitatively assessed following the instructions provided by the Nanjing JianCheng Bioengineering Institute kit.

2.7. Pyroptotic cell staining

After PAECs were treated with BDE-209, Nano-Se and 4-PBA, Hoechst and PI/Annexin V-FITC mixed staining was performed according to Miao et al. (2022). The Hoechst staining solution (Beyotime Biotechnology Co., LTD., Shanghai, China) was incubated at an ice bath temperature for 30 min, then washed with PBS, and subsequently incubated with a mixture of PI and Annexin V-FITC (Sevin Innovation Biotechnology Co., LTD., Beijing, China) for 20 min. Finally, fluorescence microscopy (Thermo Fisher Scientific, USA). was employed to evaluate the extent of pyroptosis damage.

2.8. Immunofluorescence (IF)

PAECs were treated with BDE-209, Nano-Se and 4-PBA. Subsequently, they were fixed in 4 % paraformaldehyde overnight at 4 °C. The next day, they were washed with TBSTx for 15 min and then incubated with TBSTx containing 5 % bovine serum albumin (BSA, BioFroxx, Germany) for 60 min. Primary antibodies, including TXNIP (1:2000, ABclon Biotech, China) and GSDMD (1:2000, ABclon Biotech, China), were incubated overnight at 4 °C. After washing, fluorescent secondary antibodies were applied, consisting of Alexa Fluor 488-conjugated sheep anti-rabbit IgG (1:1000, Biodragon, China) and DyLight 594-conjugated sheep anti-rabbit IgG (1:1000, Biodragon, China). Following another round of washing, nuclear staining was performed using DAPI, and fluorescence images were captured using a fluorescence microscope (Thermo Fisher Scientific, USA).

2.9. Determination of mRNA content by qRT-PCR

Total RNA was extracted from chicken cardiovascular tissue and PAECs using Trizol reagent (BioFlux, USA) (Cui et al., 2023). Subsequently, cDNA was synthesized from 2 to 5 μg of total RNA using Superscript II reverse transcriptase (Bloar Technology, China). qRT-PCR was carried out using the Light Cycler®480 System (BIOER, China). In this study, ERS-related genes (glucose regulatory protein 78 (GRP78), inositol need enzyme 1(IRE1), activated transcription factor 6 (ATF6), C/EBP homologous protein (CHOP) and PERK), TXNIP and pyroptosis related genes (Caspase-1, ASC, NLRP3, IL-18 and IL-1β) were detected. The primer sequence of qRT-PCR was designed and synthesized by Shanghai Engineering, with β-actin serving as the internal control. The primers used are listed in Table 1.

2.10. Determination of protein content by western blot (WB)

Total proteins of chicken cardiovascular tissues and PAECs were extracted with 10 μL phenylmethane sulfonyl fluoride (PMSF) (TransGern Biotech, China) and 100 μL the RIPA Lysis Buffer (TransGern Biotech, China). After mixing completely on ice for 30 min, centrifuge at 4 °C, 12,000 rpm for 10 min. The supernatant was taken after centrifugation, and the protein concentration was determined with the BCA protein determination kit (Solarbio, China). SDS was then added proportionally to the supernatant (sample: SDS = 4:1) and the sample was boiled for 10 min. The 12–15 % sodium dodecyl sulphate-polyacrylamide gel electrophoresis (SDS-PAGE) was used, and the protein bands were then transferred to a polyvinylidene fluoride (PVDF) film in a TRIS-Glycine buffer. Then it is enclosed in a 37 °C shaker with 5 % skim milk for 2 h. The antibodies were proportioning to dilute GRP78 (1:1500 Wanlei Biotechnology, China), IRE1 (1:1500), ATF6 (1:1000), PERK (1:1200), CHOP (1:8000 Immunoway, China), TXNIP (1:1000 ABMART Biotechnology), GSDMD (1:1000), Caspase-1 (1:500 Wanlei Biotechnology, China), ASC (1:500), NLRP3 (1:1500) and β-actin (1:500 Abways Technology, China), and then the membranes were tested overnight at 4 °C. Then rabbit IgG secondary antibody (1:10,000, Immunoway, China) was incubated for 120 min. Image J software was applied to quantify the final exposure images, with β-actin used as the internal reference.

2.11. Statistical analysis

To ensure the accuracy of the experimental data, three independent experiments were conducted. Data processing was performed using GraphPad Prism (version 8.0; GraphPad software) to process the data. All data adopt *t*-test or one-way analysis of variance (ANOVA), obeyed normal distribution, and passed equal variance test. Quantitative data are expressed as mean ± standard deviation. A level of $p < 0.05$ was considered statistically significant, and the different letters indicate significant differences ($p < 0.05$) between two groups.

3. Results

3.1. Histopathological changes after exposure to BDE-209 and treatment with Nano-Se

In order to investigate the protective effect of Nano-Se on chicken cardiovascular tissues, we examined cardiovascular tissues treated with BDE-209 and Nano-Se using H&E staining. Firstly, pathological changes of chicken aorta were observed. It was found that, compared with the control group, the BDE-209 group displayed distinct inflammatory cell infiltration consisting of lymphocytes and monocytes within the intima. The intimal surface was irregular and protruding, and the elastic fibers were damaged. The outer membrane exhibited hyperplasia of a considerable amount of collagen fibers, leading to thickening of the vessel wall. Partial fractures were evident in both the internal and external elastic fibers, and scar tissue had formed (Fig. 1A). Conversely, compared with BDE-209 group, the symptoms of BDE-209 + Nano-Se group were alleviated, the internal and external elastic fiber fractures were reduced, and inflammatory cells were present. There was no significant difference between Nano-Se group and Control group.

Observations through SEM revealed distinct cellular characteristics under the microscope. Cells in the Control group and the Nano-Se group exhibited clear contours, a flat surface, and visible surface villi. In contrast, the BDE-209 group displayed disordered surface cells, unclear cell morphology, widened cell gaps, vanished surface villi, and an uneven surface. When compared with the BDE-209 group, the symptoms of the BDE-209 + Nano-Se group were reduced; although some cells retained an unclear shape, cell spacing was diminished, and cell

Table 1
The primers used in the present study.

Gene	Gene numbers	Primer sequence (5′ → 3′)	Primer lengths (bp)	Product lengths (bp)
β-actin	NM_205518.2	Forward: CCAGCCATGTATGTAGCCATCCAG	24	90
		Reverse: AACACCATCACCAGAGTCCATCAC	24	
GRP78	XM_040648980.2	Forward: CCTCCTGCTCCTCGTGGTGTC	21	101
		Reverse: TTGTTCCCAGTGCCTTTGTCTTCAG	25	
IRE1	XM_015294255.4	Forward: CGCCCAAAGCATCAAACCATTCTG	24	127
		Reverse: CACTCTGTTGGCATCGTCATCTCC	24	
CHOP	XM_040693765.2	Forward: TGAGCTGGATGAGACACTGAATGC	24	150
		Reverse: CGCTTCCGCTTTGTCCTCTGC	21	
ATF6	XM_052665883.1	Forward: TGCAGCTCCCAGATGTCTCCTATC	24	100
		Reverse: TGACGCCCACAATCGGTTTCTTC	23	
PERK	XM_040671515.2	Forward: GGGCGAGGATGTTGTCTTAGTTGG	24	90
		Reverse: GCCGAGCAGATGTACTTCACCTTC	24	
TXNIP	XM_040690680.2	Forward: ATCAACGCCGACTTCGAGAACAC	23	150
		Reverse: CATGCCCGAGATGATGTGGTTACC	24	
Caspase-1	XM_015295935.4	Forward: TCGGATGGCTGGAGATGTGTAGAG	24	104
		Reverse: GAGACAGTGTCAGGCGTGGAAG	22	
ASC	NM_001040467.1	Forward: ACAACAAGTCGGAGCAGTACATCG	24	108
		Reverse: CAGCCACCTCATACGCCTTCTTC	23	
NLRP3	NM_001348947.2	Forward: GCTCCTTGCGTGCTCTAAGACC	22	150
		Reverse: TTGTGCTTCCAGATGCCGTCAG	22	
IL-18	XM_015297948.4	Forward: CAAAGTGCCAGTGAACCCCAGAC	23	86
		Reverse: ACAGAGAGGGTCACAGCCAGTC	22	
IL-1β	XM_046931582.1	Forward: CTTCATCTTCTACCGCCTGGACAG	24	133
		Reverse: CTGGTCGGGTTGGTTGGTGATG	22	

adhesion was observed on the surface (Fig. 1B). Furthermore, TEM showed that the Control group displayed elliptical or circular nuclei, normal chromatin distribution, and typical mitochondrial morphology and arrangement. In the BDE-209 group, cell membrane perforations disrupted membrane integrity, resulting in chromatin and contents overflowing and a fragmented appearance. Intracellular prominences and cytoplasmic debris were evident, signifying cell damage and pyroptosis induced by BDE-209. The addition of Nano-Se improved cell damage (Fig. 1C).

3.2. Effects of BDE-209 exposure and Nano-Se treatment on the survival rate of PAECs

To further substantiate the hypothesis that the mechanism of BDE-209-induced cardiovascular tissue injury might be related to the TXNIP-NLRP3 pathway through ERS, we conducted in vitro experiments using cultured PAECs. Subsequently, we prepared solutions of BDE-209 (Fig. 3D), Nano-Se(Fig. 3E) and 4-PBA (Fig. 3F) with varying concentration gradients. The outcomes revealed a decrease in cell survival rate with increasing BDE-209 concentration. In this experiment, the survival rate of cells treated with 100 mg/ml of BDE-209 was approximately 80 %. While lower concentrations of Nano-Se appeared to enhance cell growth, the cell survival rate declined when concentrations exceeded 4 μmol/L. For this study, cells treated with 4 μmol/L of Nano-Se were selected. As the concentration of 4-PBA increased, the cell survival rate decreased, with the final selected concentration being 0.5 mmol/L, resulting in a survival rate of about 95 %.

3.3. Effects of BDE-209 and Nano-Se treatments on the antioxidant capacity of cardiovascular tissue in chickens and PAECs

PAECs treated with BDE-209, Nano-Se, and 4-PBA were subjected to DCFH-DA staining to validate intracellular ROS production. The findings revealed that PAECs treated with BDE-209 exhibited elevated ROS production, whereas Nano-Se and 4-PBA were effective in reducing ROS production (Fig. 2A) ($P < 0.05$). The levels of T-AOC, MDA, SOD, and CAT in chicken cardiovascular tissue and PAECs were analyzed to assess their antioxidant capacity. The outcomes indicated a decrease in T-AOC, SOD, and CAT levels, coupled with an increase in MDA levels. In summary, BDE-209 exposure led to the induction of OS in both chicken cardiovascular tissue and PAEC cells, while Nano-Se and 4-PBA demonstrated the ability to effectively mitigate BDE-209-induced OS (Fig. 2B-C) ($P < 0.05$).

3.4. Nano-Se inhibited the expression of PAECs ERS gene and protein in chicken cardiovascular endothelial tissue induced by BDE-209

We examined mRNA expression of the ERS-related genes GRP78, IRE1, ATF6, PERK, and CHOP in tissues and PAECs. The qRT-PCR results showed that, compared with the Control group, the expressions of GRP78, IRE1,ATF6, CHOP and PERK were increased by 172.33 %, 161.83 %, 153.51 %, 272.22 % and 149.05 %, respectively, in the BDE-209 group. While the expression levels in the BDE-209 + Nano-Se group were lower than those in the BDE-209 group but higher than those in the control group (Fig. 3A) ($P < 0.05$). The same trend was observed at the protein level (Fig. 3B-C). After adding 4-PBA to PAECs, the mRNA expression of target gene in each group was detected again. The results showed that compared with NC group, the expressions of GRP78, IRE1, ATF6, CHOP and PERK in BDE-209 group were increased by 4.47, 5.06, 1.83, 6.04 and 3.50 folds, respectively. Compared with the BDE-209 group, the gene expression in the BDE-209 + 4-PBA group and BDE-209 + Nano-Se group was decreased, and the decreased expression in the BDE-209 + 4-PBA + Nano-Se group was the largest, but higher than that in the Control group (Fig. 3D) ($P < 0.05$). The same trend was observed at the protein level (Fig. 3E-F).

3.5. Nano-Se inhibited BDE-209-induced expression of TXNIP genes and proteins in chicken cardiovascular endothelial tissue and PAECs

The mRNA expression of BDE-209 group in chicken vascular tissues was significantly higher than that of Control group (Fig. 4A) ($P < 0.05$). Compared with the Control group, TXNIP protein expression in BDE-209 group was significantly increased, and TXNIP protein expression was decreased in BDE-209 + Nano-Se group, but higher than that in the Control group (Fig. 4B-C). After adding 4-PBA to PAECs, the expression trend of TXNIP mRNA in BDE-209 group was the same as in tissues. Compared with the BDE-209 group, the gene expression levels of the BDE-209 + Nano-Se group and BDE-209 + 4-PBA group were decreased, and the TXNIP gene expression levels in the BDE-209 + 4-PBA + Nano-Se group were also significantly decreased, but higher than that in NC group (Fig. 4D) ($P < 0.05$). The same trend was observed at the protein level (Fig. 4E-F).

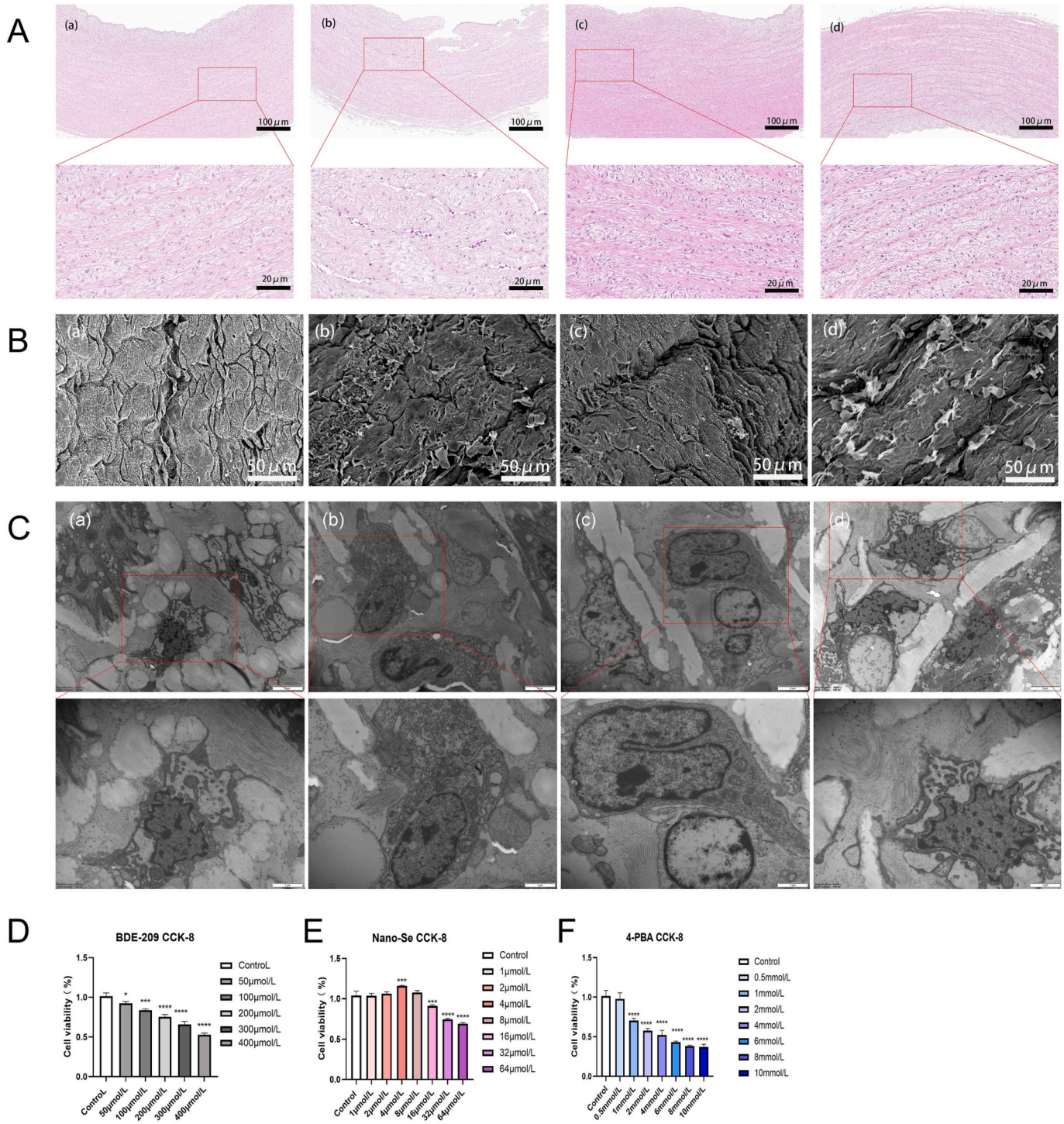

Fig. 1. Histopathological analysis of chicken cardiovascular tissue. A Hematoxylin and Eosin staining. Below is the extension of the red box in the above fig. B scanning electron microscope. C The vascular tissue was observed using a transmission electron microscope. Below is the extension of the red box in the above figure. (a) control group, (b) Decabromodiphenyl ether (BDE-209) group, (c) Nano-selenium (Nano-Se) group and (d) BDE-209 + Nano-Se group. D—F The Cell Counting Kit-8 assay to assess the cell viability of Chicken arterial endothelial cells (PAECs) following treatment with various concentrations of BDE-209, 4-PBA and Nano-Se for 12 h.

3.6. Nano-Se inhibits BDE-209 induced pyroptosis of chicken vascular tissue and PAECs

The mRNA expression levels of Caspase-1, ASC, NLRP3, IL-18 and IL-1β were detected by qRT-PCR. The results showed that the expression levels of all genes in BDE-209 group were higher than those in Control group. The level of related genes in BDE-209 + Nano-Se group was lower than that in BDE-209 group, but higher than that in Control group. The addition of Nano-Se alleviates this trend. (Fig. 5E) ($P < 0.05$). The results for proteins showed the same trend as for tissues (Fig. 5F-G).

We then investigated whether pyroptosis occurs in PAECs after exposure to BDE-209. PAECs were treated by Hoechst, PI and Annexin V-FITC mixed staining. The results showed that BDE-209 exposure promoted the swelling of the cell membrane and a large number of bubbles

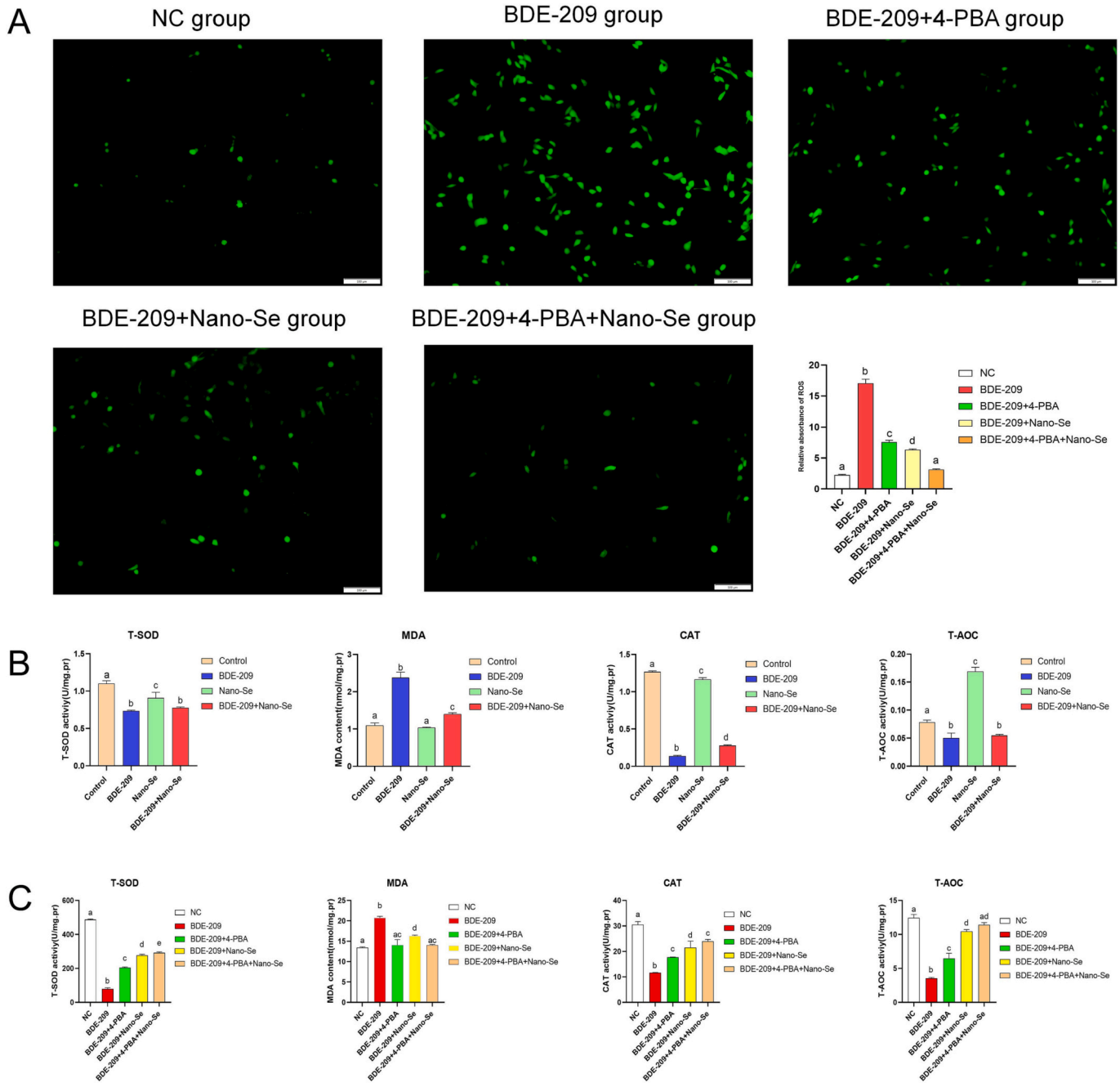

Fig. 2. A Quantification of reactive oxygen species fluorescence in PAECs. B-C total antioxidant capacity (T-AOC), malondialdehyde (MDA), superoxide dismutase (SOD), and catalase (CAT) are detected to evaluate the effects of BDE-209 and Nano-Se treatment on the antioxidant capacity of chicken cardiovascular tissue and PAECs.

appeared on the membrane surface, which was a significant morphological change of pyroptosis of cells, and Nano-Se treatment reduced pyroptosis of cells (Fig. 5A). We performed anti-TXNIP and anti-GSDMD double IF staining (Fig. 5B) and performed quantitative analysis. The results showed that after exposure to BDE-209, PAECs significantly up-regulated the expression of TXNIP and GSDMD, and after addition of Nano-Se, PAECs down-regulated the expression of TXNIP and GSDMD (Fig. 5C-D) ($P < 0.05$). The experiment showed that Nano-Se could reduce pyroptosis induced by BDE-209.

After adding 4-PBA to PAECs, the mRNA expression levels of genes in BDE-209 group showed the same change trend as those in tissues, and were significantly increased (Fig. 5H) ($P < 0.05$). Compared with the BDE-209 group, the gene expression in both the BDE-209 + 4-PBA group and the BDE-209 + Nano-Se group decreased, and the expression level in the BDE-209 + 4-PBA + Nano-Se group decreased to the lowest level, but was higher than that in NC group. The results for proteins showed the same trend as for tissues (Fig. 5I-J).

4. Discussion

BDE-209 is a ubiquitous pollutant in the environment (de Wit, 2002). Studies indicate the detection of residues of BDE-209 and similar components in 50 % of poultry feed (Zheng et al., 2015). BDE-209 further accumulates through the food chain, having significant implications for both human health and poultry farming (Chen and Hale, 2010). Previous studies have indicated that certain low-brominated congeners of

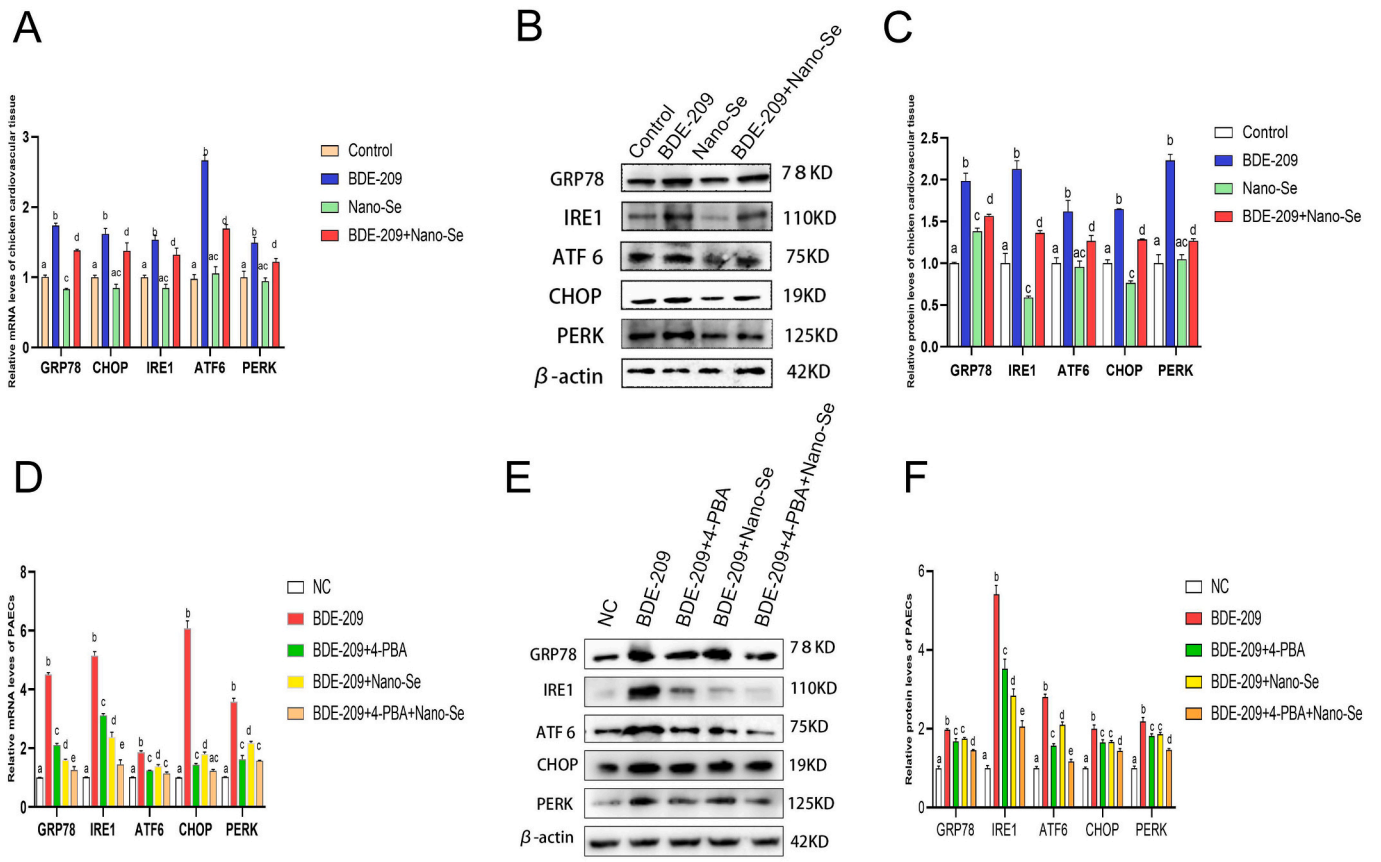

Fig. 3. Effects of BDE-209 exposure and Nano-Se intervention on endoplasmic reticulum stress (ERS) in chicken vascular tissue and PAECs. A-D ERS-related mRNA expression in chicken vascular tissues and PAECs. B-C ERS-related protein levels in chicken cardiovascular tissue. E-F ERS-related protein levels in PAECs.

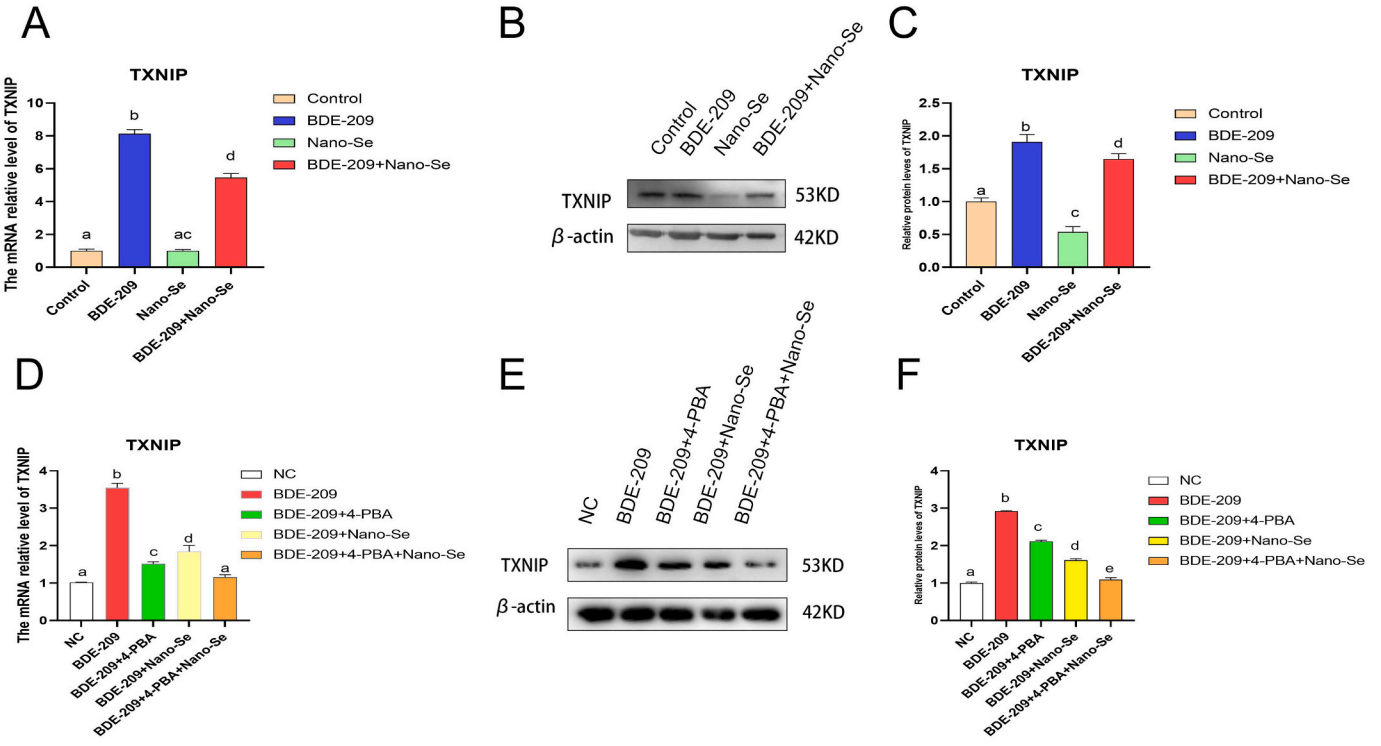

Fig. 4. Effects of BDE-209 exposure and Nano-Se intervention on thioredoxin-interacting protein (TXNIP) expression in chicken vascular tissues and PAECs. A,D Expression of TXNIP mRNA in chicken cardiovascular tissue and PAECs. B—C TXNIP protein levels in chicken cardiovascular tissue. D-E TXNIP protein levels in PAECs.

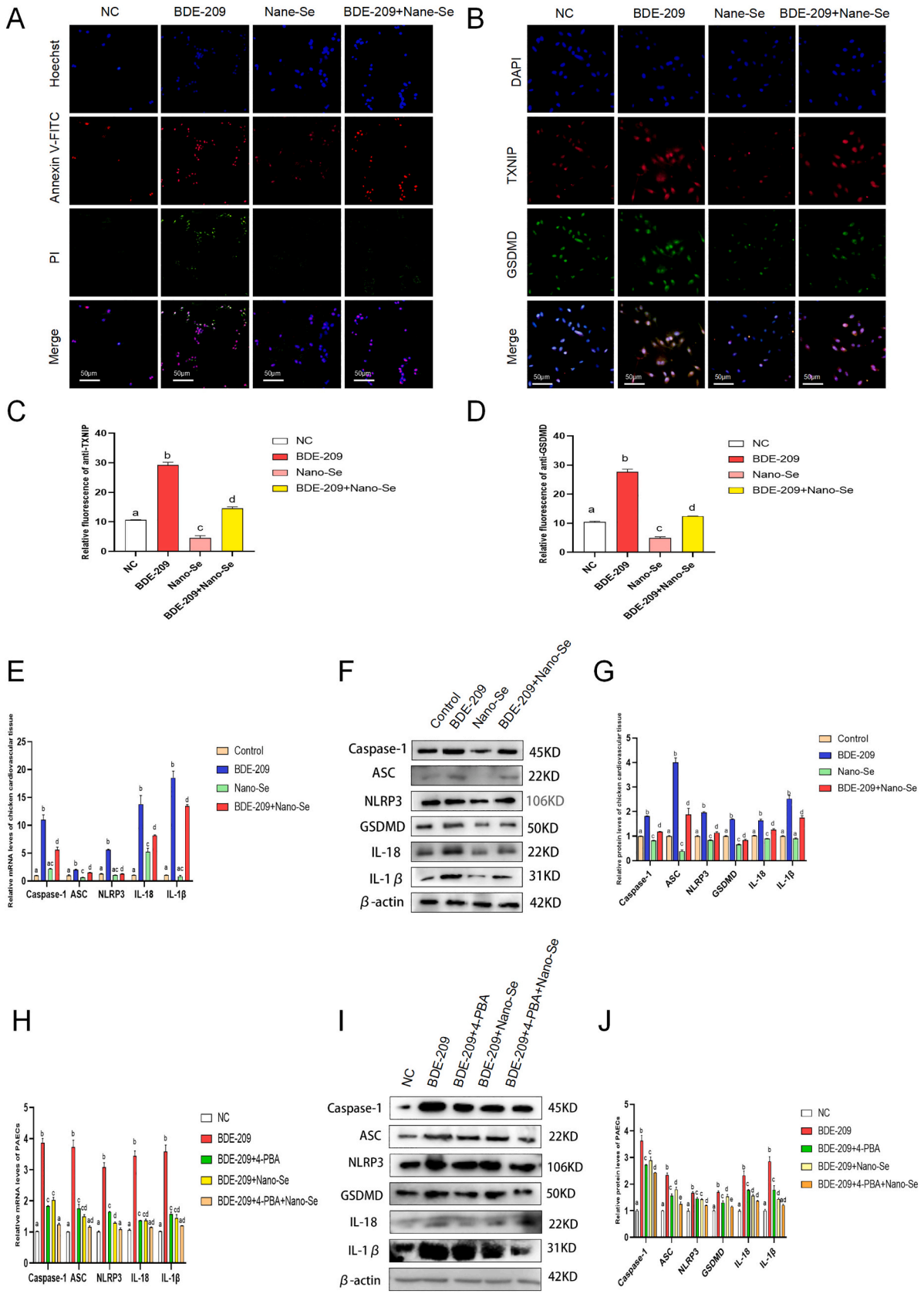

Fig. 5. Nano-Se inhibits the pyroptosis of chicken vascular tissue and PAECs induced by BDE-209. A Hoechst and PI /Annexin V-FITC mixed staining. B Immunofluorescence staining for anti-TXNIP and anti-Gasdermin-D (GSDMD) C-D TXNIP and GSDMD gene fluorescence quantitative analysis. E The mRNA express levels of pyroptosis related genes in chicken cardiovascular tissue. F-G Expression of pyroptosis related gene protein in chicken cardiovascular tissue. (H) mRNA expression of pyroptosis related genes in PAECs. I-J protein expression pyroptosis related gene in PAECs.

PBDEs are statistically correlated with certain markers of CVDs or their risk factors (Zhi et al., 2019). Zhong et al. (2019) found that exposure of zebrafish to BDE-99 hinders brain vascular growth and disrupts the formation of the blood-brain barrier by inhibiting the VEGF/VEGFR2 signaling pathway. Damage and dysfunction of vascular integrity may cause a series of CVDs (Yamagata, 2017). Several studies have highlighted the vascular toxicity of BDE-209, particularly its vascular toxicity leading to conditions like atherosclerosis and elevated blood lipids, etc. Zhi et al. (2018) and Zhi et al. (2019) found that BDE-209 not only enhances oxLDL-induced macrophage foam cell formation through increased Toll-like receptor 4 -dependent lipid uptake, but also stimulates the upregulation of intercellular adhesion molecule-1 expression, promoting monocyte adhesion to HAEC. Both mechanisms contribute to atherosclerosis development. While there have been studies on the cardiovascular effects of BDE-209, however, there is a lack of systematic research on the toxic mechanisms of BDE-209 on chicken vascular endothelium. A recent study indicated that exposure to BDE-209 induces OS and inflammatory responses in SD rats, leading to morphological and ultrastructural changes in the abdominal aorta (Jing et al., 2019). In this experiment, using 60 chickens as experimental subjects, a model of exposure to BDE-209 and Nano-Se intervention was established, yielding similar results. It was observed significant inflammatory cell infiltration among the ECs due to BDE-209 exposure. SEM revealed disordered surface cells in the BDE-209 group, with unclear cell morphology and disappearance of surface villi. In contrast, the symptoms were alleviated in the BDE-209 + Nano-Se group. Further investigation into the ultrastructural changes of vascular tissue following BDE-209 exposure revealed disrupted cell membrane integrity, leading to the overflow and fragmentation of chromatin and cellular contents. These findings suggest that BDE-209 induces vascular tissue damage and pyroptosis, while Nano-Se can alleviate its toxic effects. Nano-Se exhibits antioxidant and anti-inflammatory effects, making it a viable option for prevention and alleviation of harmful toxic effects (Sun et al., 2023). Zheng et al. (2020) indicate that Nano-Se can effectively inhibit homocysteine (Hcy)-induced mitochondrial oxidative damage and cell apoptosis in rats with hyperhomocysteinemia, both in vitro and in vivo. This helps alleviate Hcy-mediated vascular ECs damage and dysfunction. Thus, Se is regarded as a potential therapeutic approach for conditions like acute kidney injury, cardiac injury, microglial activation, and atherosclerosis (Han et al., 2021). Our research findings furnish direct evidence regarding BDE-209-induced vascular endothelial injury and inflammatory responses in chickens. These discoveries establish a theoretical foundation for delving deeper into the cardiovascular toxicity mechanisms of BDE-209, providing crucial insights for subsequent investigations.

ER homeostasis is crucial for maintaining the function and survival of vascular ECs, as well as the overall health of the body. ERS is considered to contribute to various CVDs (Ren et al., 2021). The chronic activation of ERS and the UPR pathway in ECs leads to increased OS and inflammation, often culminating in cell death (Lenna et al., 2014). An excessive protein load in the ER can trigger the dissociation of GRP78 from the UPR sensors, activating a complex network of three signaling pathways triggered by the ATF6, IRE1, and PERK sensors (Ding et al., 2023; Ayaub et al., 2016). Therefore, the activation of the aforementioned indicators is widely considered a hallmark of ERS. Hou et al. (2019) found that exposure to BDE-209 led to the upregulation of ERS markers GRP78 and IRE1α levels in HAECs, resulting in autophagy and apoptosis. Previous research has suggested that Nano-Se may alleviate granulosa cell apoptosis and mitigate the decrease in egg production induced by Hg by inhibiting the ERS pathway (Ma et al., 2022). In this study, we observed an upregulation of ERS markers in chicken vascular endothelium exposed to BDE-209. The above findings indicate that exposure to BDE-209 may induce ERS in chicken blood vessels, while supplementation with Nano-Se can restore this capability and alleviate ERS. This finding provide compelling evidence that exposure to BDE-209 induces vascular endothelial ERS in chickens, and that Nano-Se can mitigate its toxic effects.

Under ERS, the UPR response can also generate ROS that lead to cell death and inflammation (Ochoa et al., 2018; Li et al., 2023b). When there is an excess production of ROS in the body, it can lead to OS due to an imbalance between ROS generation and clearance (Sun et al., 2021). Previous studies have found that oxalate-induced kidney injury is associated with OS caused by ERS (Ming et al., 2022). Multiple studies have indicated that exposure to BDE-209 reduces antioxidant capacity (Liu et al., 2021). BDE-209 induced ferroptosis by creating OS in chicken brain (Dong et al., 2023). Moreover, the relationship between ERS and OS is bidirectional. ROS could regulate UPR signaling by reversible modifications. ERS can also regulate intracellular ROS levels (Jing et al., 2022). Research suggests that decabromodiphenyl ethane (DBDPE) exerts toxic effects on the liver in rats by inducing OS and ERS, and it may even trigger cell apoptosis (Jing et al., 2022). In rats with hypothyroidism, Nano-Se increases CAT and SOD, as well as thiol content. It reduces MDA levels in the heart and aortic tissues, exerting a protective effect on the cardiovascular system (Rastegar Moghaddam et al., 2022). The detoxifying properties of Nano-Se have the potential to enhance overall antioxidant capacity, diminish the generation of ROS, and even facilitate the clearance of ROS (Sun et al., 2023). Our results are consistent with these studies, in addition, BDE-209 decreased the levels of T-AOC, SOD, and CAT in chicken ECs, while simultaneously increasing the level of MDA. Combined with ROS staining, the results indicated a decrease in overall antioxidant capacity caused by BDE-209 exposure. Nano-Se intervention showed a partial recovery of antioxidant capacity. Similarly, the addition of 4-PBA to inhibit ERS led to a restoration of PAECs' antioxidant capacity, and the combination of Nano-Se and 4-PBA further enhanced the material's antioxidant ability. Based on the above research, we found that the cardiovascular damage caused by BDE-209 involves the participation of ERS, accompanied by OS. Nano-Se may counteract this oxidative damage.

TXNIP directly interacts with the key antioxidant protein TRX, inhibiting its antioxidant function and expression (Choi and Park, 2023). It is also associated with endothelial dysfunction and the development of atherosclerosis, and has emerged as a crucial pathological regulatory factor in CVDs (Oslowski et al., 2012; Lerner et al., 2012). Additionally, TXNIP is considered a crucial link between ERS and NLRP3 inflammasome activation (Oslowski et al., 2012). ERS interact with inflammatory mediators, triggering downstream pathways. ERS is a key inducer in the process of pyroptosis (Li et al., 2020). When cells experience irreversible ERS, TXNIP is rapidly upregulated, leading to the activation of the NLRP3 inflammasome (Lerner et al., 2012). The study by Bao et al. (2022) showed that IRE1α/TXNIP/NLRP3 inflammasome mediated by ERS plays a role in the process of liver fibrosis in diabetic mice. Xu et al. (2019) found that Apelin-13, through binding to APJ, alleviates early brain injury in an AMPK-dependent manner by inhibiting ERS-related TXNIP/NLRP3 inflammasome activation and OS in rats. ROS induce the dissociation of TXNIP from TRX, allowing its binding to NLRP3. Deficiency of TXNIP impairs the activation of the NLRP3 inflammasome and subsequent secretion of IL-1β, thereby inhibiting inflammatory responses (Zhou et al., 2010). The study has indicated that BDE-47 induces the accumulation of ROS and the expression of TXNIP, subsequently activating the NLRP3 inflammasome and promoting the secretion of mature IL-1β (Shan et al., 2018). The results of this study showed that BDE-209 up-regulated TXNIP expression, while Nano-Se inhibits its upregulation. In summary, these research findings suggest that TXNIP could be a potential target for BDE-209-induced vascular pyroptosis, and the decreased expression of TXNIP after the addition of Nano-Se may be through the induction of ERS.

Pyroptosis is a regulated pro-inflammatory form of cell death. When ECs are stimulated by exogenous substances or endogenous mediators, it can lead to OS, ERS, mitochondrial dysfunction, and immune activation. These effects may activate common signaling pathways that exacerbate endothelial dysfunction, potentially triggering the activation of the NLRP3 inflammasome (Bai et al., 2020). However, it is currently unclear

whether pyroptosis is associated with vascular damage induced by BDE-209 exposure. In recent years, several studies have reported that PBDEs can induce pyroptosis. In J774A.1 macrophages, exposure to PBDEQ induces both canonical NLRP3 inflammasome and non-canonical NLRP1 inflammasome responses, as well as pyroptosis through ROS generation and mitochondrial dysfunction (Yang et al., 2022b; Wang et al., 2021b). Zheng et al. (2021b) discovered that DBDPE may damage ECs through NLRP3 inflammasome-mediated endothelial dysfunction. However, it is currently unclear whether pyroptosis is associated with vascular damage induced by BDE-209 exposure. Our results indicate that exposure to BDE-209 and Nano-Se, Hoechst and Annexin V-FITC/PI staining results, as well as IF staining, revealed increased expression of TXNIP and GSDMD. Additionally, the expression levels of ASC, Caspase-1, GSDMD, IL-1β, and IL-18 were significantly elevated. These results showed that BDE-209 induced pyroptosis and that pyroptosis was alleviated after the addition of Nano-Se. Nano-Se can directly or indirectly inhibit the activity of the NLRP3 inflammasome (Wang et al., 2022). Se supplementation may mitigate inflammation by downregulating some pro-inflammatory genes, including NLRP3, thereby improving the antioxidant defense against atherosclerosis (Roshanravan et al., 2022). Therefore, we hypothesize that BDE-209 induces vascular endothelial injury through the ERS-TXNIP-NLRP3 pathway.

To verify whether BDE-209 induces pyroptosis through the ERS-TXNIP-NLRP3 pathway, this study introduced 4-PBA into the PAECs BDE-209 exposure model. The results showed that 4-PBA inhibited the expression of ERS-related genes such as ATF6, IRE1, and PERK, and decreased ROS levels. Furthermore, the combined use of Nano-Se and 4-PBA exhibited a more pronounced inhibitory effect on ERS, indicating that Nano-Se enhanced the suppression of ERS. Moreover, inhibition of ERS activity led to a decrease in the expression of TXNIP and NLRP3 and reduced pyroptosis. The reason for this might be the inhibition of ERS, leading to a reduction in ROS generation, preventing the separation of TXNIP from TRX, and subsequently, the activation of the NLRP3 inflammasome. In conclusion, these findings suggest that the intervention of Nano-Se in BDE-209-induced pyroptosis occurs through the ERS-TXNIP-NLRP3 pathway.

However, there are certain limitations in our study as well. The specific pathways through which BDE-209 modulates ER remain unclear. Additionally, further research is needed to explore the relationship between BDE-209-induced ERS and OS. To address these gaps, our future efforts will involve targeted interventions within the ERS and OS process using a variety of approaches. These will enable us to conduct in-depth investigations into the intricate regulatory interplay between ERS and pyroptosis, ultimately providing a deeper understanding of the toxic mechanisms underlying BDE-209-induced effects.

5. Conclusion

The results of this study indicate that BDE-209 exposure can induce vascular endothelial injury in chickens by promoting ERS, OS, and pyroptosis. The mechanism underlying this effect might involve the disruption of ER homeostasis by BDE-209, leading to exacerbated OS, activation of TXNIP-NLRP3 inflammasome, and subsequent initiation of pyroptosis. Nano-Se, as a potential mitigator, effectively reducing the adverse impacts of BDE-209 on the cardiovascular system. These findings provide novel insights into the cardiovascular toxicity of BDE-209 and offer empirical support for strategies to alleviate its toxic effects.

Funding

This study was supported by the Natural Science Foundation of Heilongjiang Province of China (YQ2021C021) and “2023 Young Leading Talents” Project of Northeast Agricultural University (NEAU2023QNLJ-012).

CRediT authorship contribution statement

Yangyang Jiang: Writing – review & editing, Methodology, Conceptualization. **Bowen Dong:** Formal analysis, Data curation. **Xing Jiao:** Formal analysis, Data curation. **Jianhua Shan:** Validation, Software, Methodology. **Cheng Fang:** Validation, Software, Methodology. **Kaixuan Zhang:** Validation, Software, Methodology. **Di Li:** Writing – review & editing. **Chenchen Xu:** Writing – review & editing. **Ziwei Zhang:** Resources, Methodology, Conceptualization.

Declaration of competing interest

The authors declare that they have no known competing financial interests or personal relationships that could have appeared to influence the work reported in this paper.

Data availability

Data will be made available on request.

References

Ayaub, E.A., Kolb, P.S., Mohammed-Ali, Z., Tat, V., Murphy, J., Bellaye, P.-S., Shimbori, C., Boivin, F.J., Lai, R., Lynn, E.G., Lhoták, Š., Bridgewater, D., Kolb, M.R., Inman, M.D., Dickhout, J.G., Austin, R.C., Ask, K., 2016. GRP78 and CHOP modulate macrophage apoptosis and the development of bleomycin-induced pulmonary fibrosis. J. Pathol. 239 (4), 411–425.

Bai, B., Yang, Y., Wang, Q., Li, M., Tian, C., Liu, Y., Aung, L.H.H., Li, P.-F., Yu, T., Chu, X.-M., 2020. NLRP3 inflammasome in endothelial dysfunction. Cell Death Dis. 11 (9), 776.

Bao, X., Li, J., Ren, C., Wei, J., Lu, X., Wang, X., Du, W., Jin, X., Ma, B., Zhang, Q., Ma, B., 2022. Aucubin ameliorates liver fibrosis and hepatic stellate cells activation in diabetic mice via inhibiting ER stress-mediated IRE1α/TXNIP/NLRP3 inflammasome through NOX4/ROS pathway. Chem. Biol. Interact. 365, 110074.

Cai, S.J., Wu, C.X., Gong, L.M., Song, T., Wu, H., Zhang, L.Y., 2012. Effects of nano-selenium on performance, meat quality, immune function, oxidation resistance, and tissue selenium content in broilers. Poult. Sci. 91 (10), 2532–2539.

Cai, J., Guan, H., Jiao, X., Yang, J., Chen, X., Zhang, H., Zheng, Y., Zhu, Y., Liu, Q., Zhang, Z., 2021. NLRP3 inflammasome mediated pyroptosis is involved in cadmium exposure-induced neuroinflammation through the IL-1β/IkB-α-NF-κB-NLRP3 feedback loop in swine. Toxicology 453, 152720.

Cai, J., Liu, P., Zhang, X., Shi, B., Jiang, Y., Qiao, S., Liu, Q., Fang, C., Zhang, Z., 2023. Micro-algal astaxanthin improves lambda-cyhalothrin-induced necroptosis and inflammatory responses via the ROS-mediated NF-κB signaling in lymphocytes of carp (Cyprinus carpio L.). Fish Shellfish Immunol. 139, 108929.

Cao, C., Fan, R., Chen, M., Li, X., Xing, M., Zhu, F., Xue, H., Wang, K., Xu, S., 2018. Inflammatory response occurs in veins of broiler chickens treated with a selenium deficiency diet. Biol. Trace Elem. Res. 183 (2), 361–369.

Chen, D., Hale, R.C., 2010. A global review of polybrominated diphenyl ether flame retardant contamination in birds. Environ. Int. 36 (7), 800–811.

Chen, X., Guo, X., Ge, Q., Zhao, Y., Mu, H., Zhang, J., 2019. ER stress activates the NLRP3 inflammasome: a novel mechanism of atherosclerosis. Oxidative Med. Cell. Longev. 2019, 3462530.

Chen, S., Che, S., Li, S., Wan, J., Ruan, Z., . High-fat diet exacerbated decabromodiphenyl ether-induced hepatocyte apoptosis via intensifying the transfer of Ca2+ from endoplasmic reticulum to mitochondria. Environ. Pollut. *292* (Pt A), 118297.

Cheng, L., Rao, Q., Zhang, Q., Song, W., Guan, S., Jiang, Z., Wu, T., Zhao, Z., Song, W., 2022. The immunotoxicity of decabromodiphenyl ether (BDE-209) on broiler chicks by transcriptome profiling analysis. Ecotoxicol. Environ. Saf. 232, 113284.

Chi, Q., Zhang, Q., Lu, Y., Zhang, Y., Xu, S., Li, S., 2021. Roles of selenoprotein S in reactive oxygen species-dependent neutrophil extracellular trap formation induced by selenium-deficient arteritis. Redox Biol. 44, 102003.

Choi, E.-H., Park, S.-J., 2023. TXNIP: a key protein in the cellular stress response pathway and a potential therapeutic target. Exp. Mol. Med. 55 (7), 1348–1356.

Cui, J., Xu, T., Lv, H., Guo, M.-Y., 2023. Zinc deficiency causes oxidative stress, endoplasmic reticulum stress, apoptosis and inflammation in hepatocytes in grass carp. Fish Shellfish Immunol. 139, 108905.

Ding, L., Liao, T., Yang, N., Wei, Y., Xing, R., Wu, P., Li, X., Mao, J., Wang, P., 2023. Chrysin ameliorates synovitis and fibrosis of osteoarthritic fibroblast-like synoviocytes in rats through PERK/TXNIP/NLRP3 signaling. Front. Pharmacol. 14, 1170243.

Dong, B., Jiang, Y., Shi, B., Zhang, Z., Zhang, Z., 2023. Selenomethionine alleviates decabromodiphenyl ether-induced oxidative stress and ferroptosis via the NRF2/GPX4 pathway in the chicken brain. J. Hazard. Mater. 465, 133307.

Fang, Y., Tian, S., Pan, Y., Li, W., Wang, Q., Tang, Y., Yu, T., Wu, X., Shi, Y., Ma, P., Shu, Y., 2020. Pyroptosis: a new frontier in cancer. Biomed. Pharmacother. 121, 109595.

Ge, J., Guo, K., Zhang, C., Talukder, M., Lv, M.-W., Li, J.-Y., Li, J.-L., 2021. Comparison of nanoparticle-selenium, selenium-enriched yeast and sodium selenite on the

alleviation of cadmium-induced inflammation via NF-kB/IκB pathway in heart. Sci. Total Environ. 773, 145442.
Ge, J., Guo, K., Huang, Y., Morse, P.D., Zhang, C., Lv, M.-W., Li, J.-L., 2022. Comparison of antagonistic effects of nanoparticle-selenium, selenium-enriched yeast and sodium selenite against cadmium-induced cardiotoxicity via AHR/CAR/PXR/Nrf2 pathways activation. J. Nutr. Biochem. 105, 108992.
Goodman, J.E., 2009. Neurodevelopmental effects of decabromodiphenyl ether (BDE-209) and implications for the reference dose. Regul. Toxicol. Pharmacol. 54 (1).
Han, Y., Lu, Y., Li, X., Niu, X., Chang, A.K., Yang, Z., Li, X., He, X., Bi, X., 2021. Novel organoselenides (NSAIDs-Se derivatives) protect against LPS-induced inflammation in microglia by targeting the NOX2/NLRP3 signaling pathway. Int. Immunopharmacol. 101 (Pt B), 108377.
He, Y., Peng, L., Zhang, W., Liu, C., Yang, Q., Zheng, S., Bao, M., Huang, Y., Wu, K., 2018. Adipose tissue levels of polybrominated diphenyl ethers and breast cancer risk in Chinese women: a case-control study. Environ. Res. 167, 160–168.
Hetz, C., Chevet, E., Harding, H.P., 2013. Targeting the unfolded protein response in disease. Nat. Rev. Drug Discov. 12 (9), 703–719.
Hites, R.A., 2004. Polybrominated diphenyl ethers in the environment and in people: a meta-analysis of concentrations. Environ. Sci. Technol. 38 (4), 945–956.
Hou, Y., Fu, J., Sun, S., Jin, Y., Wang, X., Zhang, L., 2019. BDE-209 induces autophagy and apoptosis via IRE1α/Akt/mTOR signaling pathway in human umbilical vein endothelial cells. Environ. Pollut. *253*, 429–438.
Huang, H., Chen, J., Sun, Q., Liu, Y., Tang, Y., Teng, X., 2021. NLRP3 inflammasome is involved in the mechanism of mitigative effect of selenium on lead-induced inflammatory damage in chicken kidneys. Environ. Sci. Pollut. Res. Int. 28 (9), 10898–10908.
Ji, T., Han, Y., Yang, W., Xu, B., Sun, M., Jiang, S., Yu, Y., Jin, Z., Ma, Z., Yang, Y., Hu, W., 2019. Endoplasmic reticulum stress and NLRP3 inflammasome: crosstalk in cardiovascular and metabolic disorders. J. Cell. Physiol. 234 (9), 14773–14782.
Jing, L., Sun, Y., Wang, Y., Liang, B., Chen, T., Zheng, D., Zhao, X., Zhou, X., Sun, Z., Shi, Z., 2019. Cardiovascular toxicity of decabrominated diphenyl ethers (BDE-209) and decabromodiphenyl ethane (DBDPE) in rats. Chemosphere 223, 675–685.
Jing, L., Sun, Y., Wang, J., Zhou, X., Shi, Z., 2022. Oxidative stress and endoplasmic reticulum stress contributed to hepatotoxicity of decabromodiphenyl ethane (DBDPE) in L-02 cells. Chemosphere 286 (Pt 1), 131550.
Jing, L., Zheng, D., Sun, X., Shi, Z., 2023. DBDPE upregulates NOD-like receptor signaling to induce NLRP3 inflammasome-mediated HAECs pyroptosis. Environ. Pollut. 318, 120882.
Lenna, S., Han, R., Trojanowska, M., 2014. Endoplasmic reticulum stress and endothelial dysfunction. IUBMB Life 66 (8), 530–537.
Lerner, A.G., Upton, J.-P., Praveen, P.V.K., Ghosh, R., Nakagawa, Y., Igbaria, A., Shen, S., Nguyen, V., Backes, B.J., Heiman, M., Heintz, N., Greengard, P., Hui, S., Tang, Q., Trusina, A., Oakes, S.A., Papa, F.R., 2012. IRE1α induces thioredoxin-interacting protein to activate the NLRP3 inflammasome and promote programmed cell death under irremediable ER stress. Cell Metab. 16 (2), 250–264.
Li, M., Liu, Z., Gu, L., Yin, R., Li, H., Zhang, X., Cao, T., Jiang, C., 2014. Toxic effects of decabromodiphenyl ether (BDE-209) on human embryonic kidney cells. Front. Genet. 5, 118.
Li, N., Zhou, H., Wu, H., Wu, Q., Duan, M., Deng, W., Tang, Q., 2019. STING-IRF3 contributes to lipopolysaccharide-induced cardiac dysfunction, inflammation, apoptosis and pyroptosis by activating NLRP3. Redox Biol. 24, 101215.
Li, W., Cao, T., Luo, C., Cai, J., Zhou, X., Xiao, X., Liu, S., 2020. Crosstalk between ER stress, NLRP3 inflammasome, and inflammation. Appl. Microbiol. Biotechnol. 104 (14), 6129–6140.
Li, X., Liu, J., Zhou, G., Sang, Y., Zhang, Y., Jing, L., Shi, Z., Zhou, X., Sun, Z., 2021. BDE-209 and DBDPE induce male reproductive toxicity through telomere-related cell senescence and apoptosis in SD rat. Environ. Int. 146, 106307.
Li, B., Huo, S., Du, J., Zhang, X., Zhang, J., Wang, Q., Song, M., Li, Y., 2023a. Dibutyl phthalate causes heart damage by disrupting Ca2+ transfer from endoplasmic reticulum to mitochondria and triggering subsequent pyroptosis. Sci. Total Environ. 892, 164620.
Li, D., Zhang, K., Xu, C., Jiang, Y., Shan, J., Zhang, Z., Cai, J., 2023b. Cypermethrin induces apoptosis, autophagy and inflammation via ERS-ROS-NF-κB axis in hepatocytes of carp (Cyprinus carpio). Pestic. Biochem. Physiol. 196, 105625.
Lind, P.M., van Bavel, B., Salihovic, S., Lind, L., 2012. Circulating levels of persistent organic pollutants (POPs) and carotid atherosclerosis in the elderly. Environ. Health Perspect. 120 (1), 38–43.
Liu, Z., Lei, H., Tang, R., Yang, J., Guo, X., Huang, R., Rao, Q., Cheng, L., Zhao, Z., . Effects of decabrominated diphenyl ether exposure on growth, meat characteristics and blood profiles in broilers. Animals (Basel) *11* (2).
Ma, Y., Cheng, B., Li, Y., Wu, Q., Wang, Y., Chai, X., Ren, A., 2022. Protective effect of nano-selenium on mercury-induced prehierarchical follicular atresia in laying hens. Poult. Sci. 101 (12), 102190.
Maharjan, P., Martinez, D.A., Weil, J., Suesuttajit, N., Umberson, C., Mullenix, G., Hilton, K.M., Beitia, A., Coon, C.N., 2021. Review: physiological growth trend of current meat broilers and dietary protein and energy management approaches for sustainable broiler production. Animal 15 (Suppl. 1), 100284.
Meng, T., Cheng, J., Tang, Z., Yin, H., Zhang, M., 2021. Global distribution and trends of polybrominated diphenyl ethers in human blood and breast milk: a quantitative meta-analysis of studies published in the period 2000-2019. J. Environ. Manag. 280, 111696.
Miao, Z., Miao, Z., Teng, X., Xu, S., 2022. Melatonin alleviates lead-induced intestinal epithelial cell pyroptosis in the common carps (Cyprinus carpio) via miR-17-5p/TXNIP axis. Fish Shellfish Immunol. 131, 127–136.
Ming, S., Tian, J., Ma, K., Pei, C., Li, L., Wang, Z., Fang, Z., Liu, M., Dong, H., Li, W., Zeng, J., Peng, Y., Gao, X., 2022. Oxalate-induced apoptosis through ERS-ROS-NF-κB signalling pathway in renal tubular epithelial cell. Mol. Med. 28 (1), 88.
Ochoa, C.D., Wu, R.F., Terada, L.S., 2018. ROS signaling and ER stress in cardiovascular disease. Mol. Asp. Med. 63, 18–29.
Oslowski, C.M., Hara, T., O'Sullivan-Murphy, B., Kanekura, K., Lu, S., Hara, M., Ishigaki, S., Zhu, L.J., Hayashi, E., Hui, S.T., Greiner, D., Kaufman, R.J., Bortell, R., Urano, F., 2012. Thioredoxin-interacting protein mediates ER stress-induced β cell death through initiation of the inflammasome. Cell Metab. 16 (2), 265–273.
Pan, J., Han, L., Guo, J., Wang, X., Liu, D., Tian, J., Zhang, M., An, F., 2018. AIM2 accelerates the atherosclerotic plaque progressions in ApoE−/− mice. Biochem. Biophys. Res. Commun. 498 (3), 487–494.
Rastegar Moghaddam, S.H., Hosseini, M., Sabzi, F., Hojjati Fard, F., Marefati, N., Beheshti, F., Darroudi, M., Ebrahimzadeh Bideskan, A., Anaeigoudari, A., 2022. Cardiovascular protective effect of nano selenium in hypothyroid rats: protection against oxidative stress and cardiac fibrosis. Clin. Exp. Hypertens. 44 (3), 268–279.
Ren, J., Bi, Y., Sowers, J.R., Hetz, C., Zhang, Y., 2021. Endoplasmic reticulum stress and unfolded protein response in cardiovascular diseases. Nat. Rev. Cardiol. 18 (7), 499–521.
Roshanravan, N., Koche Ghazi, M.K., Ghaffari, S., Naemi, M., Alamdari, N.M., Shabestari, A.N., Mosharkesh, E., Soleimanzadeh, H., Sadeghi, M.T., Alipour, S., Bastani, S., Tarighat-Esfanjani, A., 2022. Sodium selenite and Se-enriched yeast supplementation in atherosclerotic patients: effects on the expression of pyroptosis-related genes and oxidative stress status. Nutr. Metab. Cardiovasc. Dis. 32 (6), 1528–1537.
Shan, Q., Zheng, G.-H., Han, X.-R., Wen, X., Wang, S., Li, M.-Q., Zhuang, J., Zhang, Z.-F., Hu, B., Zhang, Y., Zheng, Y.-L., 2018. Troxerutin protects kidney tissue against BDE-47-induced inflammatory damage through CXCR4-TXNIP/NLRP3 signaling. Oxidative Med. Cell. Longev. 2018, 9865495.
Shao, B.-Z., Xu, Z.-Q., Han, B.-Z., Su, D.-F., Liu, C., 2015. NLRP3 inflammasome and its inhibitors: a review. Front. Pharmacol. 6, 262.
Sun, S., Jin, Y., Yang, J., Zhao, Z., Rao, Q., 2021. Nephrotoxicity and possible mechanisms of decabrominated diphenyl ethers (BDE-209) exposure to kidney in broilers. Ecotoxicol. Environ. Saf. 208, 111638.
Sun, X.-H., Lv, M.-W., Zhao, Y.-X., Zhang, H., Ullah Saleem, M.A., Zhao, Y., Li, J.-L., 2023. Nano-selenium antagonized cadmium-induced liver fibrosis in chicken. J. Agric. Food Chem. 71 (1), 846–856.
Sutterwala, F.S., Ogura, Y., Szczepanik, M., Lara-Tejero, M., Lichtenberger, G.S., Grant, E.P., Bertin, J., Coyle, A.J., Galán, J.E., Askenase, P.W., Flavell, R.A., 2006. Critical role for NALP3/CIAS1/Cryopyrin in innate and adaptive immunity through its regulation of caspase-1. Immunity 24 (3), 317–327.
Tang, J., Hu, B., Zheng, H., Qian, X., Zhang, Y., Zhu, J., Xu, G., Chen, D., Jin, X., Li, W., Xu, L., 2021. 2,2′,4,4'-Tetrabromodiphenyl ether (BDE-47) activates aryl hydrocarbon receptor (AhR) mediated ROS and NLRP3 inflammasome/p38 MAPK pathway inducing necrosis in cochlear hair cells. Ecotoxicol. Environ. Saf. 221, 112423.
Wan, R., Li, X., Zha, Y., Zheng, X., Huang, H., Li, M., 2022. Short- and long-term effects of decabromodiphenyl ether (BDE-209) on sediment denitrification using a semi-continuous microcosm. Environ. Pollut. 293, 118589.
Wang, J.-X., Bao, L.-J., Shi, L., Liu, L.-Y., Zeng, E.Y., 2019. Characterizing PBDEs in fish, poultry, and pig feeds manufactured in China. Environ. Sci. Pollut. Res. Int. 26 (6), 6014–6022.
Wang, J., Yan, Z., Zheng, X., Wang, S., Fan, J., Sun, Q., Xu, J., Men, S., 2021a. Health risk assessment and development of human health ambient water quality criteria for PBDEs in China. Sci. Total Environ. 799, 149353.
Wang, Y., Fang, C., Xu, L., Yang, B., Song, E., Song, Y., 2021b. Polybrominated diphenyl ether quinone exposure induces atherosclerosis progression via CD36-mediated lipid accumulation, NLRP3 inflammasome activation, and pyroptosis. Chem. Res. Toxicol. 34 (9), 2125–2134.
Wang, S., Chen, Y., Han, S., Liu, Y., Gao, J., Huang, Y., Sun, W., Wang, J., Wang, C., Zhao, J., 2022. Selenium nanoparticles alleviate ischemia reperfusion injury-induced acute kidney injury by modulating GPx-1/NLRP3/Caspase-1 pathway. Theranostics 12 (8), 3882–3895.
de Wit, C.A., 2002. An overview of brominated flame retardants in the environment. Chemosphere 46 (5), 583–624.
Xing, X., Kang, J., Qiu, J., Zhong, X., Shi, X., Zhou, B., Wei, Y., 2018. Waterborne exposure to low concentrations of BDE-47 impedes early vascular development in zebrafish embryos/larvae. Aquat. Toxicol. 203, 19–27.
Xu, W., Li, T., Gao, L., Zheng, J., Yan, J., Zhang, J., Shao, A., 2019. Apelin-13/APJ system attenuates early brain injury via suppression of endoplasmic reticulum stress-associated TXNIP/NLRP3 inflammasome activation and oxidative stress in a AMPK-dependent manner after subarachnoid hemorrhage in rats. J. Neuroinflammation 16 (1), 247.
Yamagata, K., 2017. Docosahexaenoic acid regulates vascular endothelial cell function and prevents cardiovascular disease. Lipids Health Dis. 16 (1), 118.
Yang, Y., Li, J., Han, T.-L., Zhou, X., Qi, H., Baker, P.N., Zhou, W., Zhang, H., 2020. Endoplasmic reticulum stress may activate NLRP3 inflammasomes via TXNIP in preeclampsia. Cell Tissue Res. 379 (3), 589–599.
Yang, Y., Zhu, X., Rao, Q., Liu, Z., Yang, J., Zhao, Z., 2022a. Toxicokinetics and edible tissues-specific bioaccumulation of decabrominated diphenyl ethers (BDE-209) after exposure to the broilers. Ecotoxicol. Environ. Saf. 248, 114324.
Yang, B., Wang, Y., Fang, C., Song, E., Song, Y., 2022b. Polybrominated diphenyl ether quinone exposure leads to ROS-driven lysosomal damage, mitochondrial dysfunction and NLRP3 inflammasome activation. Environ. Pollut. *311*, 119846.
Yang, Y., Jin, Y., Zhu, X., Rao, Q., Zhao, Z., Yang, J., 2023. Hepatotoxicity evaluation and possible mechanisms of decabrominated diphenyl ethers (BDE-209) in broilers:

oxidative stress, inflammatory, and transcriptomics. Ecotoxicol. Environ. Saf. 264, 115460.
Yu, G., Bu, Q., Cao, Z., Du, X., Xia, J., Wu, M., Huang, J., 2016. Brominated flame retardants (BFRs): a review on environmental contamination in China. Chemosphere 150, 479–490.
Zhang, Y., Zhang, J., Bao, J., Tang, C., Zhang, Z., 2021. Selenium deficiency induced necroptosis, Th1/Th2 imbalance, and inflammatory responses in swine ileum. J. Cell. Physiol. 236 (1), 222–234.
Zhang, Z., Shan, J., Shi, B., Dong, B., Wu, Q., Zhang, Z., 2023. SeNPs alleviates BDE-209-induced intestinal damage by affecting necroptosis, inflammation, intestinal barrier and intestinal flora in layer chickens. Ecotoxicol. Environ. Saf. 262, 115336.
Zhao, Y., Fan, K., Zhu, Y., Zhao, Y., Cai, J., Jin, L., 2022. Gestational exposure to BDE-209 induces placental injury via the endoplasmic reticulum stress-mediated PERK/ATF4/CHOP signaling pathway. Ecotoxicol. Environ. Saf. 233, 113307.
Zheng, X.-B., Luo, X.-J., Zheng, J., Zeng, Y.-H., Mai, B.-X., 2015. Contaminant sources, gastrointestinal absorption, and tissue distribution of organohalogenated pollutants in chicken from an e-waste site. Sci. Total Environ. 505, 1003–1010.
Zheng, Z., Liu, L., Zhou, K., Ding, L., Zeng, J., Zhang, W., 2020. Anti-oxidant and anti-endothelial dysfunctional properties of nano-selenium in vitro and in vivo of hyperhomocysteinemic rats. Int. J. Nanomedicine 15, 4501–4521.
Zheng, Y., Zhang, B., Guan, H., Jiao, X., Yang, J., Cai, J., Liu, Q., Zhang, Z., 2021a. Selenium deficiency causes apoptosis through endoplasmic reticulum stress in swine small intestine. Biofactors 47 (5), 788–800.
Zheng, D., Shi, Z., Yang, M., Liang, B., Zhou, X., Jing, L., Sun, Z., 2021b. NLRP3 inflammasome-mediated endothelial cells pyroptosis is involved in decabromodiphenyl ethane-induced vascular endothelial injury. Chemosphere 267.
Zhi, H., Wu, J.-P., Lu, L.-M., Li, Y., Chen, X.-Y., Tao, J., Mai, B.-X., 2018. Decabromodiphenyl ether (BDE-209) enhances foam cell formation in human macrophages via augmenting toll-like receptor 4-dependent lipid uptake. Food Chem. Toxicol. 121, 367–373.
Zhi, H., Wu, J.-P., Lu, L.-M., Zhang, X.-M., Chen, X.-Y., Wu, S.-K., Tao, J., Mai, B.-X., 2019. Decarbromodiphenyl ether (BDE-209) promotes monocyte-endothelial adhesion in cultured human aortic endothelial cells through upregulating intercellular adhesion molecule-1. Environ. Res. 169, 62–71.
Zhong, X., Kang, J., Qiu, J., Yang, W., Wu, J., Ji, D., Yu, Y., Ke, W., Shi, X., Wei, Y., 2019. Developmental exposure to BDE-99 hinders cerebrovascular growth and disturbs vascular barrier formation in zebrafish larvae. Aquat. Toxicol. 214, 105224.
Zhou, R., Tardivel, A., Thorens, B., Choi, I., Tschopp, J., 2010. Thioredoxin-interacting protein links oxidative stress to inflammasome activation. Nat. Immunol. 11 (2), 136–140.
Zhu, Y., Li, X., Liu, J., Zhou, G., Yu, Y., Jing, L., Shi, Z., Zhou, X., Sun, Z., 2019. The effects of decabromodiphenyl ether on glycolipid metabolism and related signaling pathways in mice. Chemosphere 222, 849–855.